

Finite Mass Simulation Techniques in LS-DYNA®

Ben Tutt¹ and Scott Roland²
Airborne Systems North America, Santa Ana, CA, 92704

and

Richard D. Charles³ and Gregory Noetscher⁴
U.S. Army Natick Soldier Research, Development, and Engineering Center (NSRDEC), Natick, MA, 01760

This paper describes the development and results of numerical models describing parachute inflation behavior. The models were developed using Fluid Structure Interaction (FSI) techniques in the commercially available transient dynamic finite element code LS-DYNA. Prior to 2009, FSI simulation methodologies developed at Airborne Systems had restricted analysis to the steady-descent phase of parachute operations. That is to say the modeling was performed in an infinite mass scenario, where the parachute does not influence the freestream air velocity; such models can be compared to tests conducted in a wind tunnel or during the steady descent phase of operation. Funding provided by NSRDEC in 2009/10 enabled Airborne Systems to develop a simulation methodology that is capable of assessing parachute performance in a finite mass scenario. Such a scenario enables the more complex inflation phase of a parachute to be investigated. In addition, the availability of experimental data, describing parachute inflation, has until recently proved limiting in quantifying the accuracy of simulation techniques. The availability of test data from a series of indoor vertical parachute tests conducted at the Space Power Facility at NASA Glenn Research Center Plum Brook Station provided an excellent means of code result validation. The experimental test set-up produced a sufficiently controlled and instrumented environment specifically developed for basic parachute performance data collection. The results of the modeling, discussed herein, compare favorably with the indoor vertical parachute tests, with good prediction of both inflation force and post inflation breathing frequency. The models were developed prior to test data reduction and analysis, and as such acted as a true prediction.

Nomenclature

C_d	= Drag coefficient
D_0	= Nominal diameter
PIA	= Parachute Industries Association

¹ Systems Analyst, Airborne Systems, 3000 Segerstrom Ave, Santa Ana, CA 92704. AIAA Senior Member.

² Systems Analyst, Airborne Systems, 3000 Segerstrom Ave, Santa Ana, CA 92704. AIAA Member.

³ Research Aerospace Engineer, U.S. Army RDECOM, NSRDEC, Natick, MA 01760. AIAA Associate Fellow.

⁴ Electrical Engineer, U.S. Army RDECOM, NSRDEC, Natick, MA 01760. AIAA Member.

I. Introduction

In 2004, Airborne Systems (then Irvin Aerospace) initiated a strategy to develop an analysis methodology that enabled parachutes to be simulated in a virtual environment. The objective was to provide an additional tool to the parachute designer that could enhance the understanding of parachute performance and guide future design decisions. A simulation methodology, developed by Airborne Systems in 2003, to simulate the water impact loads of a returning manned spacecraft using the transient dynamic finite element code LS-DYNA¹ highlighted the capability of the code to accurately simulate the interaction of a fluid (water, air, etc.) and a structure. An internally funded research and development study compared exhaustive testing during the Apollo program to LS-DYNA model predictions². The opportunity to demonstrate the applicability of this numerical technique for simulating parachute behavior arrived in late 2004. At the time, the XT-11 main parachute had exhibited some undesirable flight characteristics during US Army testing. An LS-DYNA model was generated that was capable of replicating those flight characteristics and subsequently identified a design modification to eliminate the glide modes³.

In 2006/7, Airborne Systems under contract to NSRDEC, refined this simulation methodology and demonstrated its applicability for a number of parachutes. A capability to assess the influence of fabric permeability on parachute performance was also developed during that contract. Airborne Systems contributed internal funding and worked with LSTC (Livermore Software Technology Corporation), the developers of LS-DYNA, to develop, integrate, and test a specific algorithm that permitted gas flow through a permeable media. This work enabled a broader range of parachutes to be investigated within the simulation methodology previously developed.

These efforts provided an engineering tool to evaluate the performance of ballistic parachutes when in steady descent or when subjected to small or medium level deformations, such deformations could be riser pulls, damage assessments, wind gusts etc. Although valuable, these techniques did not provide the parachute engineer with a method for understanding the inflation of the parachute. Parachute inflation is typically the period of operation when peak deceleration forces occur and consequently when maximum design risk is found. A capability that enabled the parachute engineer to evaluate inflation performance prior to testing could greatly reduce technical risk, eliminate unnecessary testing, and following testing help assess design margin and performance envelope. This paper describes the initial efforts to compare parachute inflation test data with numerical model predictions, and identify the next stages of development required to create a design tool.

II. Experimental Parachute Inflation Test Data

The results of the LS-DYNA numerical models were compared with experimental work conducted by NSRDEC to aid validation studies of parachute modeling in general. The particular experimental series considered throughout this report was the indoor vertical tests⁴ conducted at the Space Power Facility (SPF) at the NASA Glenn Research Center (GRC) Plum Brook Station in Sandusky, Ohio.

The test chamber at the SPF is 100 ft in diameter and 120 ft high at the center of the chamber. The facility is constructed from 1 in thick aluminum floor, walls, and ceiling, and surrounded by a 6 ft thick outer concrete structure. A photograph of the facility and schematics of the facility are shown in Figure 1. The test chamber is a circular dome-shaped structure designed for high vacuum conditions to test space hardware, although for this series of parachute tests the chamber was maintained at ambient atmospheric conditions. The semi-quiescent nature of the chamber provided an ideal environment for testing parachutes in a controlled and repeatable manner. Parachutes ranging in size from 3.5 ft to 9 ft in diameter were dropped from both packed and free-hanging configurations. A guide wire was used to limit horizontal motion and enable consistent and repeatable testing. The wire passed through the center of the payload and the parachute vent. The payloads were instrumented with four load cells, a hot-wire based anemometer and a three-axis accelerometer. In addition, photogrammetry techniques were utilized to measure the deformed shape of the parachute as a function of time using reflective markers located on the canopy fabric.

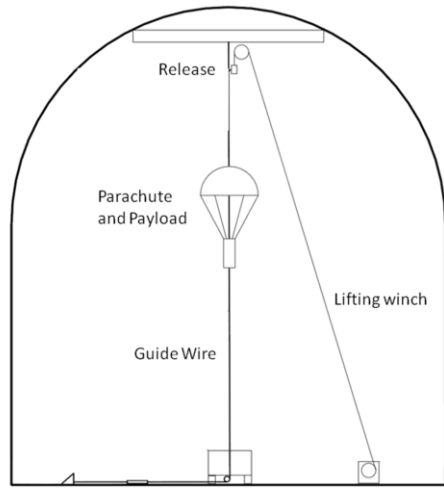
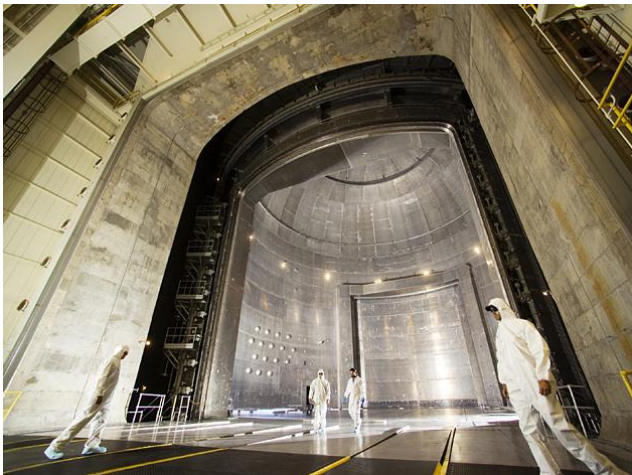


Figure 1. NASA Glenn Research Center, Plum Brook Station, Parachute Test Set-up Schematic

A. Parachute Configurations

Although data was gathered from a variety of planforms and sizes the parachutes considered for the numerical modeling study were a 7 ft nominal diameter (D_0) flat circular canopy and a 5 ft D_0 ringslot canopy. Both canopies are known to behave differently and as such present different and unique numerical challenges.

The flat circular canopy was fabricated from 1.1 oz/yd² fabric (PIA-C-7020 Type I) and the ringslot canopy was fabricated from low permeability F-111 material (PIA-C-44387 Type I).

The parachutes were released from a nominal free-hanging position from a height of 100 ft for the drops considered in this paper. Each parachute had sixteen suspension lines. The lines were collected into four groups and tension force was measured on each of these groups using independent load cells. The accelerometer was mounted inside the payload. Data was sampled from all sensors at 1000 Hz.

III. Model Development and Numerical Methodology

A. Numerical Approach

It is possible to use LS-DYNA in a number of ways to enable the interaction of a dynamic fluid and a thin membrane structure. The parachute in question and the objectives of the modeling will dictate which method is selected.

The numerical approach discussed in this paper utilizes a first order Eulerian temporal solution with a second order accurate advection method. An Eulerian formulation on a Cartesian mesh is used for the fluid, Lagrangian 4-noded membrane elements based on the Belytschko-Lin-Tsay formulation for the parachute structural mesh, and a quasi penalty based coupling method to enable the two to interact. The use of an Eulerian-Lagrangian coupling algorithm permits the interaction of the fluid and structure to occur within the same computational solver and completely avoids the numerical problems associated with distortions of the fluid mesh. Unlike previous models that force air to flow through the spatially fixed Cartesian mesh, this model contains stationary fluid and the parachute and payload move through the fluid mesh.

It is only within the last 4-5 years that this method of solving both the fluid and structure within the same code has emerged as a viable way of simulating parachute performance. The application of Eulerian formulations can lead to a propensity for energy dissipation and dispersion inaccuracies connected with the fluxing of mass across element boundaries. In addition, the Eulerian mesh is required to span the entire range of activity associated with the Lagrangian structure. In many applications, this can result in a large size mesh and hence a high computing cost. Many of these potential difficulties have been managed through algorithm development and vast improvements in computing power. Ballistic parachutes are relatively unique aerodynamic devices that are designed to generate drag and as such their bluff body form is ideally suited to Euler based solutions.

B. Modeling Strategy

The modeling strategy developed for this study is illustrated in Figure 2. This approach produced both an Indoor Vertical Test simulation, and a separate drag prediction of the parachute in a wind tunnel environment.

The drag force prediction is a result of an infinite mass, wind tunnel type simulation. The model used for this simulation constrains the payload and forces air past the parachute at a prescribed velocity. This modeling approach has been used at Airborne Systems for many years and has been the subject of past work³. It was used in this study to evaluate the modeling approaches and fluid computational mesh requirements on a smaller scale prior to undertaking the extensive finite mass simulations. The finite mass modeling path shown in Figure 2 represents the work discussed in this paper.

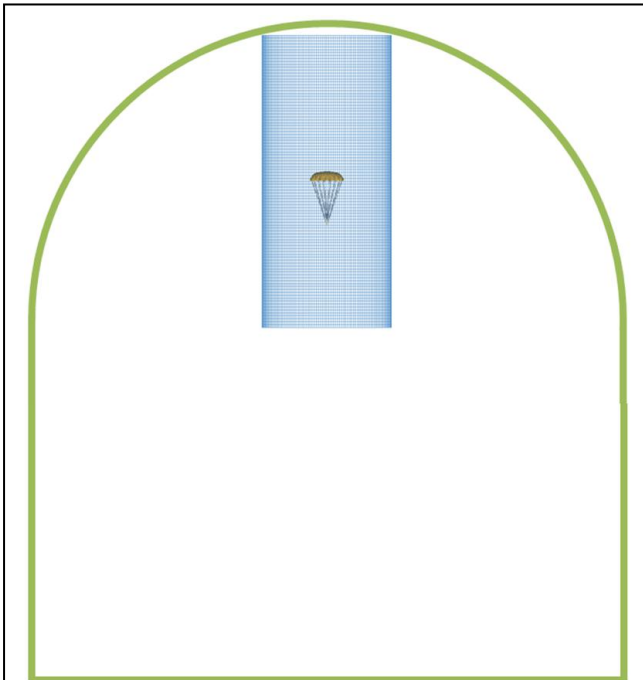


Figure 3. Relative Scale of Computational Mesh to SPF Test Chamber

The mesh sensitivity study indicated that the simulation predictions would marginally benefit from a smaller fluid element height. However, the simulation run-time became prohibitive at more than 1 million hexahedral elements. Details of the computational mesh are provided below.

Fluid Mesh:

# of Elements-	902,400 Solid Hexahedral Elements
# of Nodes-	920,817 Nodes
File Size -	146 MB

Parachute Mesh:

# of Elements-	3,392 Membrane Elements, 360 Seatbelt Elements
# of Nodes-	3,820 Nodes

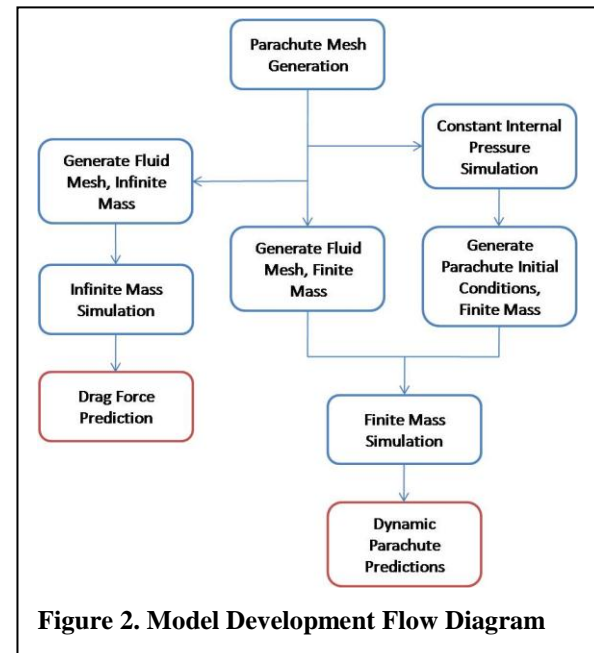


Figure 2. Model Development Flow Diagram

The Eulerian fluid mesh generated for the finite mass inflation task replicated only a small section of interest within the SPF. To construct a fluid mesh of suitable density to fill the entire volume of the test chamber would far exceed the available computational power. The purpose of this work was to evaluate the modeling methodology rather than replicate the entire drop test. Current work is assessing the developments required to improve the parallelization efficiency of this class of model.

Figure 3 illustrates the relative size of the computational mesh and the cross sectional area of the SPF. The SPF test chamber is 100 ft in diameter and 120 ft high at the center of the chamber. The computational mesh is 21.5 ft in diameter and 65 ft in height. The height of each fluid element (5 in) is constant throughout the height of the test chamber. However, a graded density profile was applied to the radial dimension of the fluid. The height of the fluid elements was the result of a mesh sensitivity study.

Previous work has identified the importance of accurately capturing the parachute construction techniques in the numerical model, with particular emphasis on the canopy fabric geometry and material angles. The inflated shape of the canopy is dependent upon incorporation of accurate material angles and dimensions within each of the gores.

In order to predict the inflation force it was critical to replicate the initial parachute canopy shape before the release of the parachute. Figure 4, reproduced from Ref 4 depicts a parachute in the free-hanging position prior to being raised to the ceiling. This required taking the known flat circular parachute planform and allowing it to deform appropriately into a representative free-hanging geometry. This had to be accomplished without inducing excessive stress and strain in the canopy that could artificially alter the canopy geometry, prior to the drop test simulation.

The approach selected was to deform the parachute structure in a separate simulation and then use that geometry as the starting shape for the drop test simulation. To enhance the overall accuracy of this method for the 7-ft flat circular canopy, the full parachute canopy was reduced to a single gore. By limiting the simulation to a single gore, the resulting parachute geometry was more symmetric and any induced fabric strains were minimized.

The single parachute canopy gore was constructed flat where the geometry of the gore could be accurately defined, as seen in Figure 5. The gore fabric was then allowed to fall under a simulated gravity loading, the radials were constrained to move only on their original plane and the apex was fully constrained. This caused the gore to fall slowly into a vertical folded shape. Several iterations of this approach, with various falling speeds, were used to ensure no permanent strains were induced in the fabric. A permanent strain would be carried forward into the finite mass simulation, and as the parachute inflated in the fluid the canopy would take an unrealistic deformed shape. Once the simulation was completed the single gore was then rotated 16 times to construct the full parachute, as illustrated in Figure 5.



Figure 4. Free-Hanging Parachute Configuration

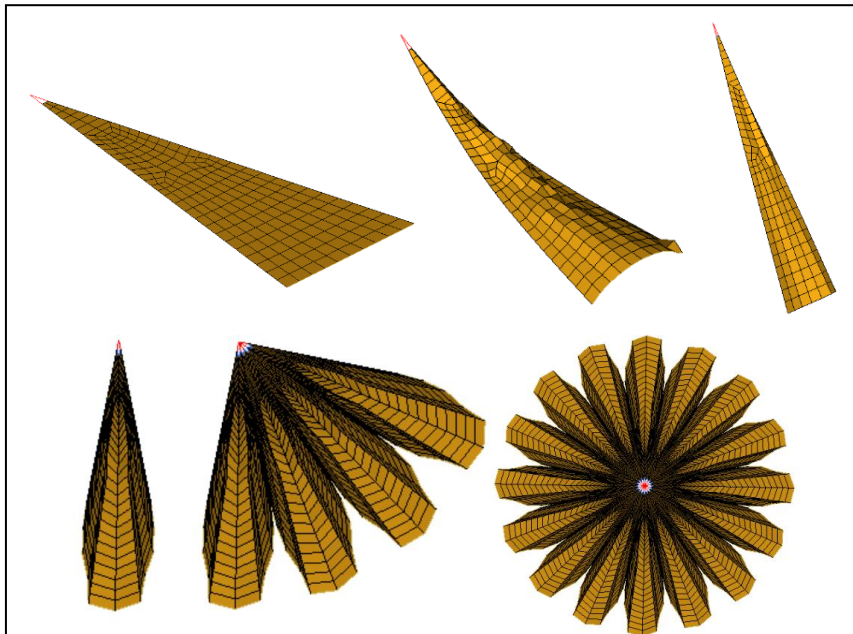


Figure 5. Flat Circular Canopy, Free Hanging Shape Generation

To sufficiently reproduce the initial opening load shock of the parachute inflation process it was necessary to capture, as accurately as possible, the initial skirt diameter. Models were generated with several different initial diameters to illustrate the influence of the free hanging skirt shape on the resulting peak inflation loading. Initial skirt diameters were achieved by modifying the inputs for the process depicted in Figure 5. Figure 6 shows the accelerations recorded at the payload as a result of both a small and a larger initial skirt diameter.

Although only two of the many initial diameter iterations are shown in Figure 6, it still clearly illustrates that the initial skirt diameter is highly critical in capturing the full inflation loads.

It also highlights that although the initial inflation loads of the two parachute simulations are different, the initial conditions by no means affect the resulting steady state conditions; as is observed in reality.

Creating the initial free-hanging state of the ringslot canopy followed the same approach but additional care had to be taken to ensure adjacent rings did not become entangled. Figure 7 illustrates the computational mesh and the steps in creating the initial deformed shape.

In addition to the initial skirt diameter study, attention was paid to the density of the fluid mesh as well as the density of the parachute mesh. Although the general make-up of the meshes was important to the overall performance of the parachute system, it proved to have less influence on the parachute inflation than the initial skirt diameter.

During the drop test experiments in the SPF the parachutes were constrained to a vertical guide wire, which partially constrained lateral movement of the canopy and payload. To replicate this quasi constraint in the simulation a pre-tensioned vertical cable was incorporated into the model. As with the drop test, the cable was allowed to slide through the payload and the center of the canopy vent. Seatbelt elements and slirings were used to replicate the guide wire function in the model. The payload and parachute were both free to move vertically and laterally, to the extent allowed by the guide wire, throughout the entire simulation.

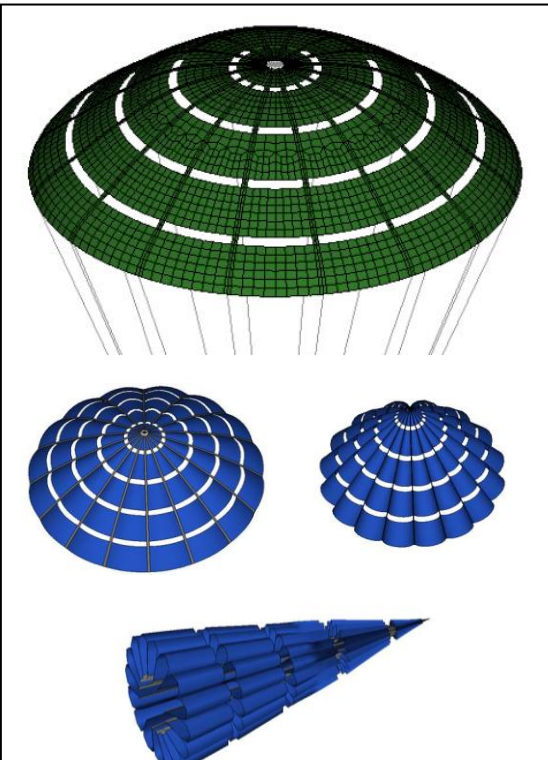


Figure 7. Ringslot Canopy, Free Hanging Shape Generation

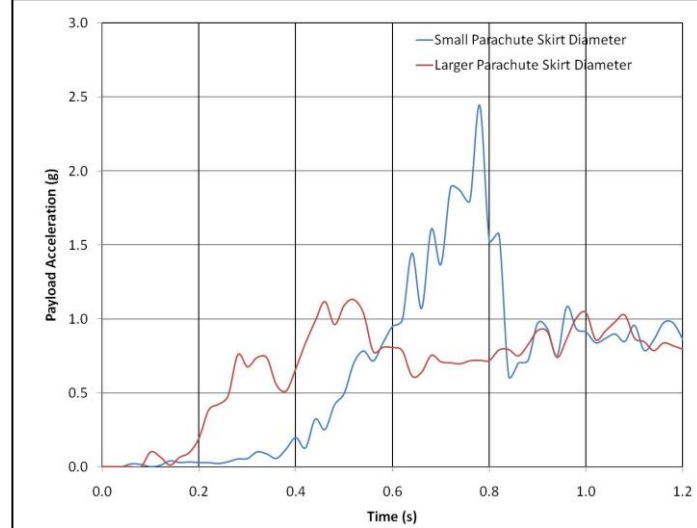


Figure 6. Influence of Initial Skirt Diameter on Payload Inflation Acceleration

Simulation results are presented for both the 7 ft flat circular and 5 ft ringslot parachute.

IV. Simulation Results

Given the dynamic nature of the inflation process, it is not possible to suitably capture it in this paper with a single screen shot. Therefore, multiple time elapsed screen shots have been assembled in Figure 8 to illustrate the inflation process. The images are shown with a perspective view to aid the spatial observation of the canopy geometry during the inflation process.

As illustrated in Figure 8, the parachute starts in its free hanging position and then rapidly inflates. It is shown to progress into an over inflation shape, almost flat, and then contract and once again over inflate. This phenomenon is often referred to as breathing or squidding. The breathing motion was most likely caused by the constraint on the motion of the parachute imposed by the guide-wire. The natural tendency of a flat circular parachute is to oscillate through a coning angle from side to side about its descent axis as it discards excess accumulated air. As this natural oscillation was restrained, the canopy appeared to expel the excess air by means of the breathing motion.

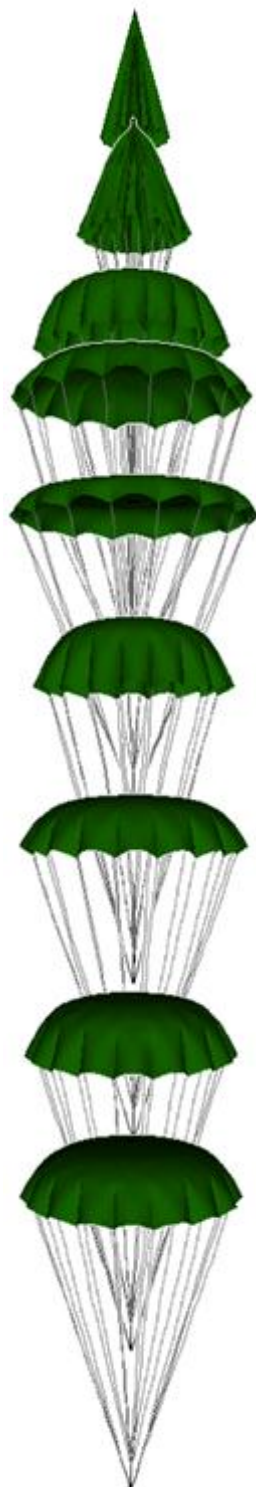


Figure 8. 5 ft Flat Circular Parachute Inflation Time Lapse Images

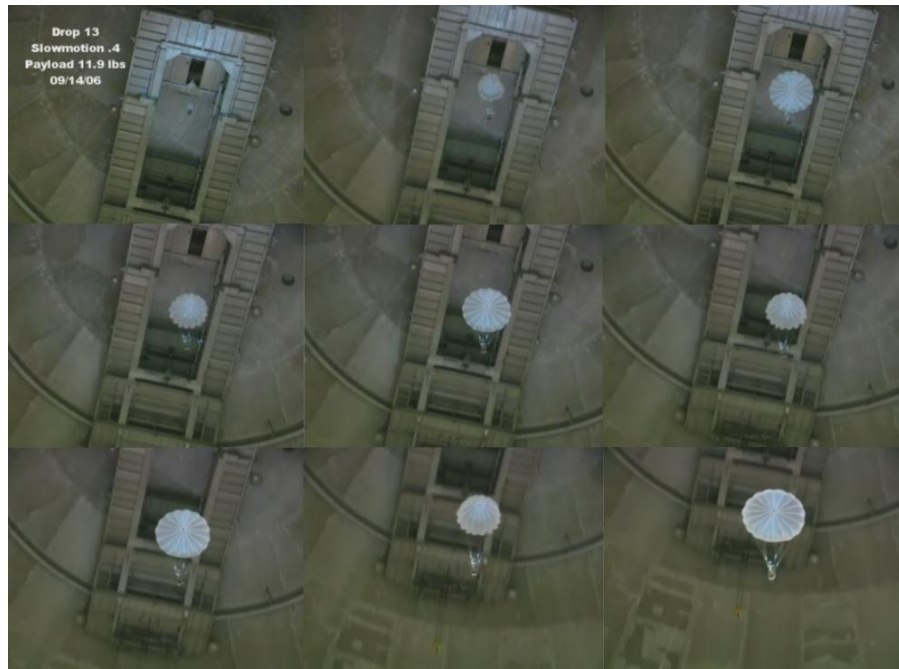


Figure 9. 5 ft Flat Circular, Frames from the Drop Test Video

For quasi comparison purposes, screen shots have been taken from an NSRDEC video of a flat circular deployment in the Plum Brook test chamber. The frames demonstrate the breathing displayed in Figure 9.

Figure 10 compares the predicted descent velocity as a function of time with the velocity measured during the drop test. The velocity measurement was taken from integrating the accelerometer output; the hot-wire based anemometer did not record accurate results for this drop test. The model under-predicts velocity by 3-8% throughout the simulation, this equates to an over-prediction of parachute drag. This difference is within the experimental variability and error bars supplied by the test team. The greatest difference in velocity is seen in the initial parachute over inflation following peak deceleration, which occurs at approximately 1.1 seconds. It is likely that this is related to the time of initial parachute operational performance (referenced

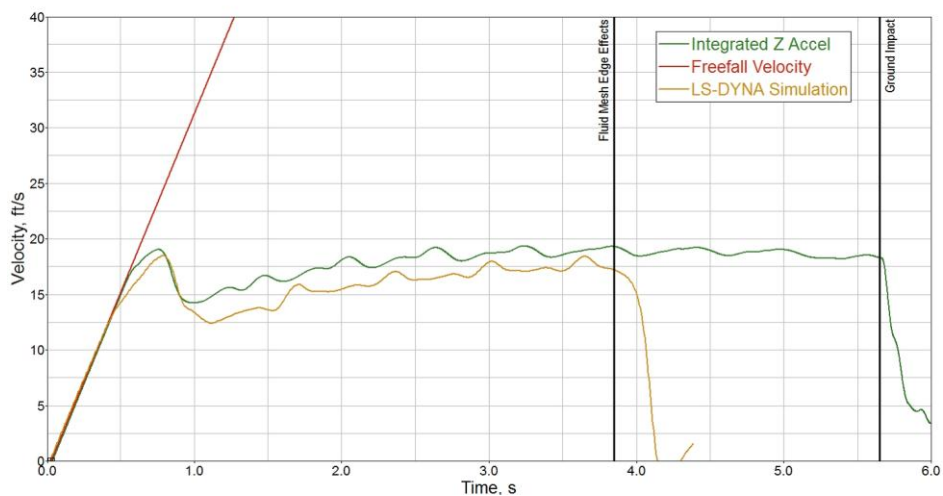


Figure 10. 5 ft Flat Circular, Descent Velocity

as the time at which the velocity first deviates from freefall velocity). As can be seen in Figure 10, the model moves from the red line prior to the drop test data and this is likely caused by a different free hanging skirt geometry of the parachute and the parachute opening marginally earlier in the model than in the test. Also noteworthy is the accurate prediction of the more complex dynamics involved, specifically the breathing exhibited as the parachute descends along the guide wire. The breathing frequency of the model and the experiment are both approximately 2 Hz. This frequency can be identified in the velocity time history data by the small increases occurring every 0.5 seconds. Also observable in both sets of data is a smaller velocity reduction that precedes the more significant velocity increase. These velocity variations represent the different phases in the breathing cycle of the parachute.

Also shown in Figure 10 is the ground impact of the payload during the test, at approximately 5.6 seconds, and the fluid mesh edge effects as the parachute reaches the bottom of the computational fluid mesh.

Not visible in any of the data provided herein is the lateral motion of the parachute as it descends down the guide wire. This lateral motion is observed in both the test data and the numerical model.

Due to computational resource restrictions the 7 ft diameter flat circular canopy finite mass drop test simulations were restricted to approximately 4.0 s of simulation time. Capturing the parachute system performance over the entire length of the drop test was deemed less of a priority than capturing the parachute performance accurately over the inflation and primary breathing cycles.

Figure 11 illustrates the fluid flow on a section through the flat circular parachute as it inflates and breathes. The time shown in the top left of each image correlates to the time scale shown in Figure 10. The top left image depicts the parachute beginning to inflate and the surrounding air remaining stationary. The nature of the inflation is interesting; it replicates the skirt first inflation observed during the drop test series. As the inflation progresses the parachute drag area increases and rapidly decelerates the payload. Throughout this time the surrounding air becomes increasingly more disturbed. As the parachute reaches its maximum projected diameter a large vortex ring is shed from the canopy skirt and the parachute then begins to contract.

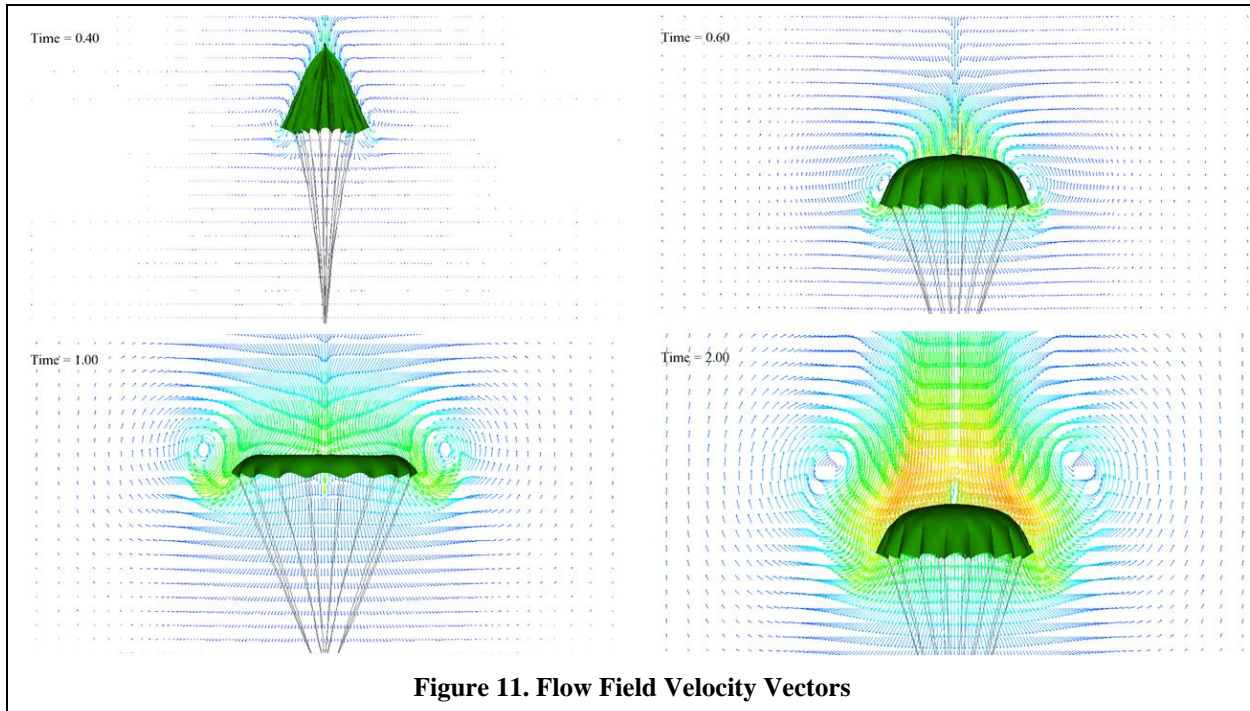


Figure 11. Flow Field Velocity Vectors

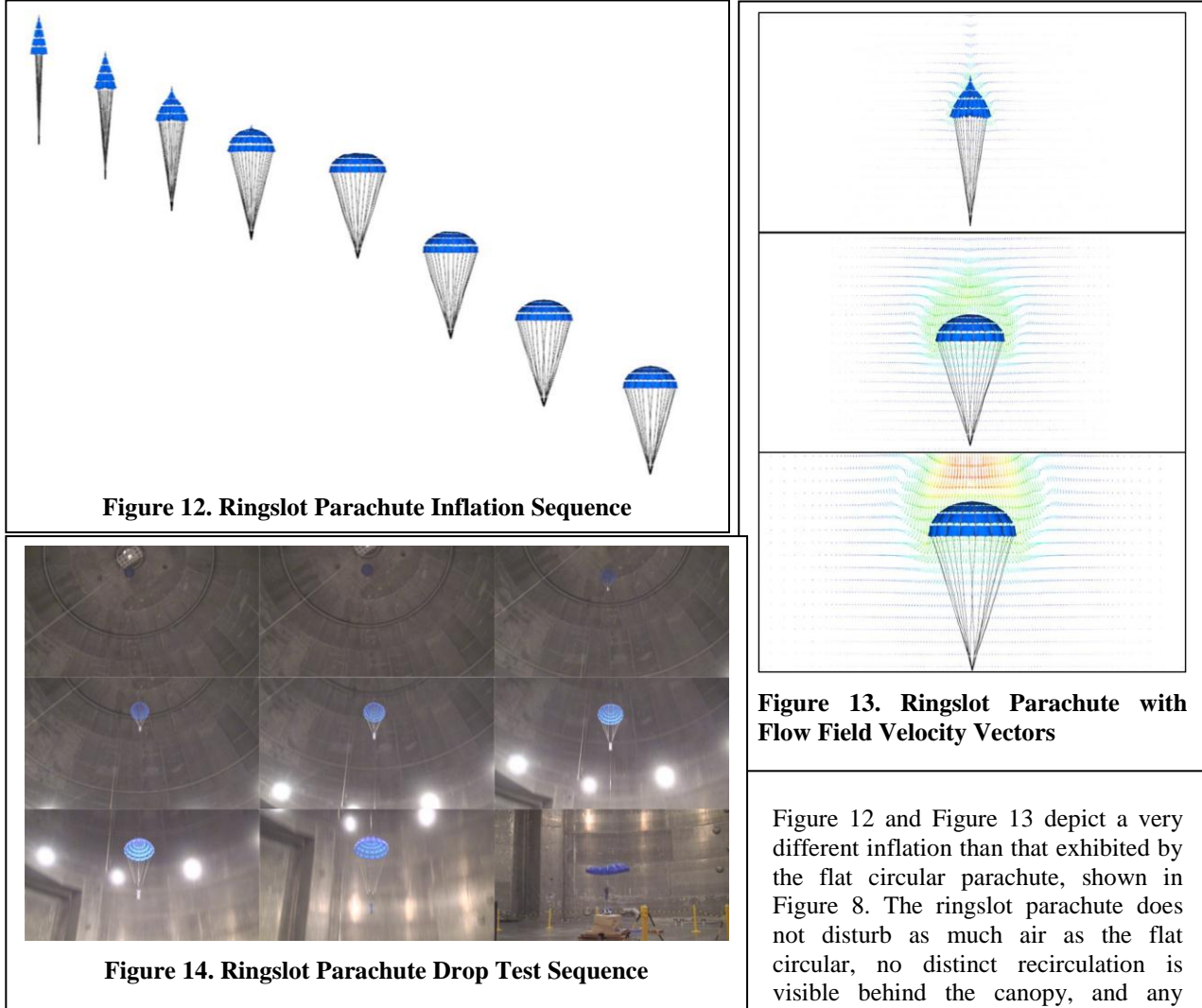
B. Ringslot Parachute

At the time of writing this paper no detailed information describing the test configuration or drop test results for the ringslot canopy was available for incorporation.

Although the canopy surface geometry was provided by NSRDEC, in order to implement that geometry into the simulation some important features needed to be incorporated. One of the more critical features was the presence of pocket bands. The pocket bands were incorporated into the parachute at the deformed initial condition, prior to inflation in the finite mass simulation. A seatbelt element was used to represent the pocket bands, each end of the

element was connected to adjacent gores at the skirt of the canopy. Each seatbelt was assigned an initial slack length to reflect the length of the actual bands on the parachute.

Figure 12 displays images of the parachute throughout the finite mass simulation. The frames are shown from left to right for clarity, and do not indicate that the parachute moved laterally. The parachute began in the free hanging position and was then released. Parachute inflation was initiated at the skirt of the canopy, air being driven in to the mouth of the canopy and forcing the bottom ring outwards. This is a different inflation sequence than those observed during actual flight operation of a ringslot canopy. A ringslot parachute is typically utilized in situations where stability is needed at high speeds and dynamic pressures. In these environments, the high speed air will move rapidly from the mouth of the canopy up to the crown before the skirt inertia can be overcome. So in actual flight operation it is less likely to observe a skirt first inflation than a crown first inflation. Also visible in Figure 12 is the relatively constant parachute diameter following inflation.



from a video of a ringslot parachute drop test, supplied by NSRDEC, are shown in Figure 14. The video recorded minimal breathing to no breathing of the canopy during a straight descent down the guide wire. No coning or oscillation was observed during the drop, however the parachute did exhibit a rotational velocity.

It was apparent in the video supplied by NSRDEC that the length of the pocket bands constricted the opening of the parachute. The bottom edge of the lowest ring appeared to form a strange rounded skirt geometry. This shape was also visible in the simulation although it is not typical of parachutes with pocket bands. The sizing of the pocket bands caused the skirt to constrict, essentially acting as a permanent reefing line. This has the potential to reduce the drag coefficient, C_d , of the canopy.

V. Conclusions

The paper has documented the preliminary stages of demonstrating the applicability of existing Fluid Structure Interaction numerical methods for predicting the inflation of parachutes. The comparisons with test data have highlighted the accuracy of the commercial finite element analysis code LS-DYNA for finite mass parachute applications. Direct quantitative comparisons have been made with descent velocity, breathing frequency, and inflation force.

The LS-DYNA model was developed after the testing had occurred but without prior knowledge of the results, as such the model outputs can be considered true predictions. The authors contend that this is an important step in the predictive capability of FSI parachute modeling in general. It is fairly common to observe good FSI model results post testing, when the results are known and have been studied in detail. It is not as common to find a predictive FSI model, especially one that compares well with complex transient test data.

The value of the data gathered from the Plum Brook drop test series has enabled the results of modeling efforts to be quantified on a level not previously available for parachute inflation studies. The testing of different planforms that exhibited distinguishing characteristics allowed the numerical processes to be tested on different levels. It is the view of the authors that the value of the test data has not been fully exhausted and that more insight can be garnered from the test series.

Model runtime is now the restrictive component of the finite mass simulation within LS-DYNA. The analysis method described herein requires the computational fluid domain to encompass the entire inflationary spatial field. This generates a large model that needs to be solved at each timestep. Current work is aimed at improving the parallelization of this specific ALE solver within LS-DYNA with the objective of considerably reducing runtime.

VI. Acknowledgments

The authors would like to acknowledge the support and funding from NSRDEC.

VII. References

¹Hallquist, J. O., "LS-DYNA Theoretical Manual," Livermore Software Technology Corporation, 1998.

²Tutt, B. A., and Taylor, A. P., "The Use of LS-DYNA to Simulate Water Entry Characteristics of Space Vehicles," 8th International LS-DYNA User's Conference, 2004.

³Tutt, B. A., et al, "The Use of LS-DYNA to Assess the Performance of Airborne Systems North America Candidate ATPS Main Parachutes," AIAA-2005-1608, 18th AIAA Aerodynamic Decelerator Systems Technology Conference and Seminar, 23-26 May 2005 Munich, Germany.

⁴Desabrais, K. J., et al, "Experimental Parachute Validation Research Program and Status Report on Indoor Drop Tests," AIAA-2007-2500, 19th AIAA Aerodynamic Decelerator Systems Technology Conference and Seminar, 21-24 May 2007 Williamsburg, Virginia.